ARTICLE

OBC
www.rsc.org/obc

Hydrogen bond directed self-assembly of core-substituted naphthalene bisimides with melamines in solution and at the graphite interface

Christoph Thalacker,[a] Atsushi Miura,[b] Steven De Feyter,*[b] Frans C. De Schryver[b] and Frank Würthner*[a]

[a] *Institut für Organische Chemie, Universität Würzburg, Am Hubland, D-97074, Würzburg, Germany. E-mail: wuerthner@chemie.uni-wuerzburg.de; Fax: +49 931 888 4756*

[b] *Department of Chemistry, Katholieke Universiteit Leuven, Celestijnenlaan 200 F, B-3001, Leuven, Belgium. E-mail: Steven.DeFeyter@chem.kuleuven.ac.be; Fax: +32 16 327990*

Received 20th September 2004, Accepted 5th November 2004
First published as an Advance Article on the web 21st December 2004

A series of red and blue highly fluorescent core-substituted naphthalene bisimide dyes has been synthesized and they have been investigated as supramolecular building blocks. NMR and UV-Vis titration experiments of these dyes with complementary melamines revealed the formation of triple hydrogen bonds (DAD–ADA arrays) in solution. At stoichiometric ratios, ditopic melamine receptors could dissolve otherwise insoluble bisimides by means of hydrogen bonding, even in aliphatic solvents. At the solution/graphite interface, one-dimensional chains of hydrogen bonded naphthalene bisimides and two-dimensional adlayers of ditopic melamines are formed for the pure compounds but little evidence for heterocomplexes between the two complementary building blocks could be obtained.

Introduction

The control of the spatial organization of functional π-systems is crucial for their application in molecular electronics, optoelectronics, photonics, sensor design and other areas of nanotechnology.[1–3] Among the functional π-systems studied so far, naphthalene and perylene bisimide dyes are particularly interesting because they combine favorable functional and structural properties.[4] From the functional point of view, these dyes are highly promising candidates for organic field effect transistors and solar cells due to their pronounced electron affinities and favorable packing properties.[2c,5] From the structural point of view, the imide positions are highly suited to direct the organization of these dyes by hydrogen bonding[6] or metal–ligand coordination,[7] which we have explored in solution for perylene bisimides in the past. Other research groups have shown by STM investigation that perylene[8] and naphthalene[9] bisimides can be deposited from the gas phase as well-defined adlayers at various surfaces and also that the supramolecular order is governed by means of hydrogen bonding between the imide units.

Our previous work has focused on perylene bisimides because these compounds are highly colored and luminescent materials in contrast to the colorless and non-fluorescent naphthalene bisimides. However, we recently discovered that naphthalene bisimides can be conveniently transformed into colored highly fluorescent dyes if amino substituents are introduced in the *ortho* position of the imide functionalities.[10] Introduction of only one amino group affords red dyes, while two amino groups provide blue dyes. Both classes of dyes exhibit intensive fluorescence with quantum yields >0.5. Accordingly, an interesting set of dyes which exhibit identical length of the supramolecular building block, but quite different optical properties, became available from the same starting material, **1**. In addition, by stepwise nucleophilic substitution of amino substituents with alkyl chains of different lengths, sterical demand or functionality can be introduced which might be applicable in the future to the control of supramolecular organization.[11] In this paper we report our first results in this direction, which include the synthesis of unsymmetrically substituted 2,6-diamino-functionalized naphthalene bisimides and their self-organization in solution, as well as at the solution/graphite interface, in the absence or in the presence of complementary melamines.[12]

Results and discussion

Synthesis

Core-substituted naphthalene bisimides bearing free imide receptor groups were obtained from 2,6-dichloronaphthalene bisanhydride **1**[13] as presented in Scheme 1.

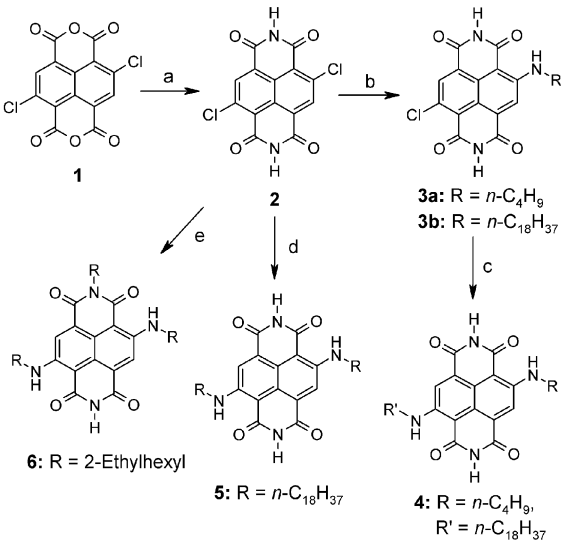

Scheme 1 Synthesis of core-substituted naphthalene bisimides **2–6**. Reagents and conditions: (a) ammonium acetate, glacial acetic acid, 120 °C, 10 min, 72%; (b) **3a**: *n*-butylamine, 25 °C, 24 h, 72%; **3b**: *n*-octadecylamine, DMF, 25–40 °C, 14 h, 70%; (c) *n*-octadecylamine, NMP, Ar, 150 °C, 1.5 h, 70%; (d) *n*-octadecylamine, Ar, 150 °C, 2 h, 52%; (e) 2-ethylhexylamine, Ar, 190 °C, 7 h, 18%.

Reaction of **1** with ammonium acetate in refluxing glacial acetic acid yielded 2,6-dichloronaphthalene bisimide **2**. Selective nucleophilic substitution of the first chlorine atom in **2** by alkylamines was achieved at temperatures below 40 °C to yield 2-chloro-6-alkylaminonaphthalene bisimides **3a,b**. The unsymmetrically substituted compound **4** and the symmetrically functionalized compound **5** were obtained from **3a** and **2**,

DOI: 10.1039/b414443k

respectively, by reaction with octadecylamine at 150 °C. To obtain monotopic imide receptor **6**, bisimide **2** was reacted with 2-ethylhexylamine at even higher temperature where a slow exchange reaction between the imide substituents takes place.[14] The low yield of **6** is due to the statistical exchange leading to significant amounts of the symmetrically substituted by-products that were separated from **6** by silica gel column chromatography. This monotopic imide receptor was synthesized for titration experiments to determine the strength of imide–melamine hydrogen bonding and the effect of hydrogen bonding on the optical properties of naphthalene bisimide dyes. The monotopic melamine receptor **7** and the ditopic melamines **8a–d** were available from our earlier work (Chart 1).[6]

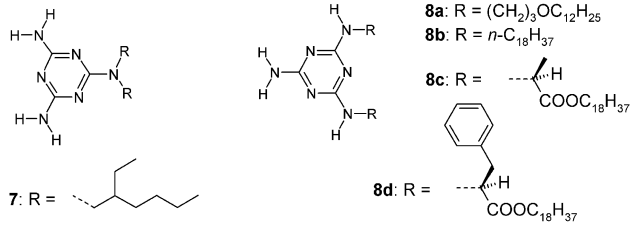

Chart 1 Monotopic melamine receptor **7** used for binding studies and ditopic melamines **8a–d** employed for experiments on superstructure formation.

Imide–melamine hydrogen bonding in solution

Imide–melamine triple hydrogen bonded assemblies have received considerable attention in supramolecular chemistry,[15] and, for many different compounds, binding constants have been determined mainly by NMR titration experiments in $CDCl_3$. In general, the binding constants for such donor–acceptor–donor (DAD) to acceptor–donor–acceptor (ADA) triple hydrogen bonding are quite modest (around 100 M^{-1})[16] and self-assembly will only afford defined larger objects if several of these units interact in a cooperative fashion, as demonstrated for double rosette assemblies by the research groups of Whitesides and Reinhoudt.[17] However, in low-polarity aliphatic solvents an appreciable increase of the binding strength of the imide–melamine triple hydrogen bond has been observed which is sufficient to trigger self-assembly in these solvents at low concentration.[6]

To evaluate the binding strength and mode of interaction for the novel amino-substituted naphthalene bisimides, titration experiments were carried out by employing the monotopic naphthalene bisimide receptor **6** and the monotopic melamine **7** (Scheme 2). As both compounds possess a high solubility, the interaction could be reliably studied in different solvents by ^{1}H NMR, UV-Vis absorption and fluorescence spectroscopy.

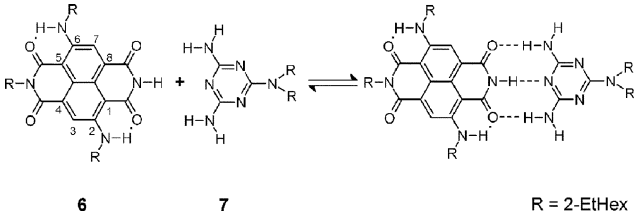

Scheme 2 Formation of a hydrogen bonded complex of 1 : 1 stoichiometry between the monotopic naphthalene bisimide **6** and melamine **7**. Note the intramolecular hydrogen bonds in **6**.

Fig. 1 shows a selection of three ^{1}H NMR spectra from the titration experiment in $CDCl_3$. In the course of the NMR titration experiment, the imide proton signal underwent a significant downfield shift of several ppm, which is characteristic of hydrogen bond formation. In addition, strong intramolecular hydrogen bonds are observed between the proton of the amino

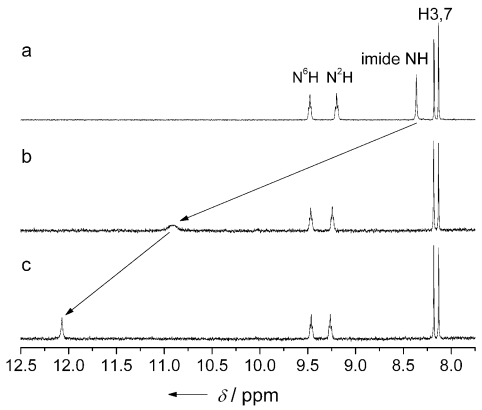

Fig. 1 ^{1}H NMR spectra (400 MHz) of solutions of **6** and **7** in $CDCl_3$. Concentration of **6**: 1×10^{-3} M, concentration of **7**: (a) 0; (b) 5.5×10^{-3} M; (c) 11×10^{-3} M.

groups (N^6H and N^2H) and the adjacent imide carbonyl oxygen. As a result, these protons appear as well-defined triplets and are significantly downfield shifted, even in DMSO, which is known for its strong hydrogen bond-breaking properties. During the NMR titration some line broadening was observed, however, the signal remained sufficiently sharp to ensure data evaluation by nonlinear regression analysis (Fig. 2).[18,19] For the proton at the amino group in 2-position, also a slight downfield shift of about 0.1 ppm was observed, indicating withdrawal of electron density from the proton upon complex formation with the melamine (Fig. 1). Evaluation of both data sets yielded the same binding constant of 130 L mol^{-1} ($\Delta G^0_{298} = -12.1$ kJ mol^{-1}). Comparison of this binding constant with those of other imide–melamine systems[6,15,16] suggests that the additional intramolecular hydrogen bond has little influence on the strength of the triple hydrogen bond DAD–ADA array. The good fit of the data, as well as a Job plot analysis, confirmed the 1 : 1 stoichiometry of the complex suggested in Scheme 2.

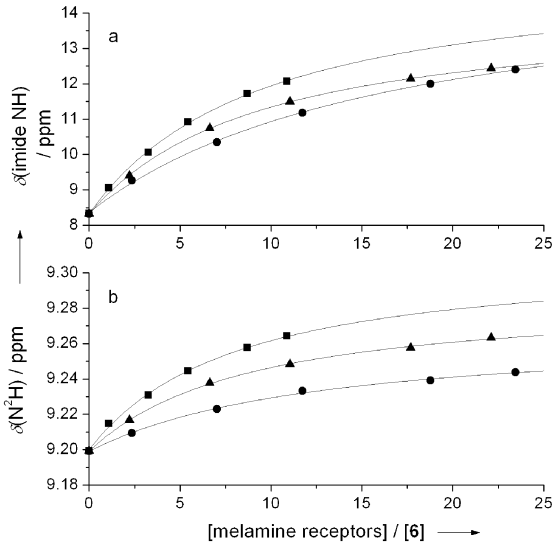

Fig. 2 ^{1}H NMR constant host titration data and calculated lines for the monotopic host **6** ($c = 1 \times 10^{-3}$ M) and melamines **7** (squares), **8b** (triangles) and **8c** (circles) in $CDCl_3$. (a) Data for imide proton; (b) data for amine N^2H proton.

For the less-polar solvent methylcyclohexane (MCH), both UV-Vis and fluorescence titration experiments were carried out. As shown in Fig. 3, only minor changes of the optical properties were observed for the naphthalene bisimide chromophore upon triple hydrogen bonding. The absorption maximum of the S_0–S_1 band at 607 nm[20] underwent a bathochromic shift of about 4 to 611 nm upon addition of the melamine and a small

increase in intensity was observed for the S_0–S_2 band between 320 and 370 nm. In addition, a small new absorption feature arises at 440 nm. In the corresponding fluorescence titration experiment, a small bathochromic shift of 4 nm was also observed for the emission maximum at 627 nm, along with a slight decrease of the integral fluorescence intensity to about 80% for the complexed naphthalene bisimide with respect to the uncomplexed chromophore. Evaluation of both data sets by nonlinear regression analysis (Fig. 4) yielded comparable binding constants that are about two orders of magnitude higher than the value in $CDCl_3$ (Table 1).

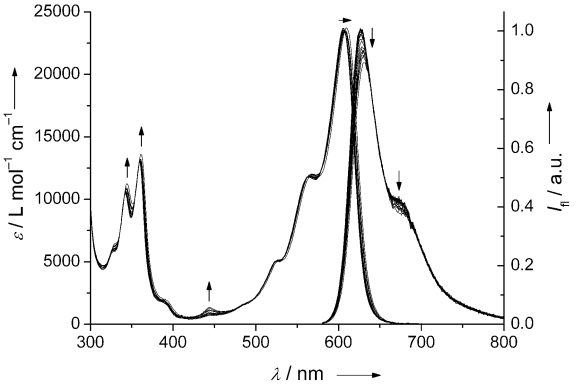

Fig. 3 Changes of the UV-Vis absorption and fluorescence spectra of monotopic naphthalene bisimide **6** (host) upon addition of melamine **7** (guest) in methylcyclohexane (host concentration 5×10^{-6} M). The arrows indicate changes upon increasing melamine concentration.

The same kind of NMR titration experiments were also carried out in $CDCl_3$ for the monotopic naphthalene bisimide **6** as the host compound and the ditopic melamines **8b** and **8c** as guests. For these systems, microscopic site binding constants of 90 and 65 M^{-1} were determined assuming two independent ADA receptor sites for the melamine. These results are in full accordance with our earlier observations for perylene imides.[6] Thus, for both imide systems the binding constants of the ditopic melamines **8b,c** are lower by a factor of about two compared to monotopic melamine **7**.[21]

Absorption and fluorescence properties of hydrogen bonded dye aggregates

Based on the binding constants in Table 1, extended hydrogen bonded assemblies between ditopic 2,6-diamino-substituted naphthalene bisimides **3–5** and ditopic melamines **8** can be only expected in solutions of aliphatic solvents. However, in these solvents none of the dyes **3–5** exhibit a reasonable solubility. Therefore, we prepared 1 : 1 complexes between these dyes and melamines **8a–d** in chloroform, subsequently evaporated this solvent and attempted to redissolve the compounds in methylcyclohexane (MCH). As shown in Table 2, only few combinations afforded colored solution and even for those precipitation of the dyes took place within a couple of hours. These results suggest that complexation of the naphthalene

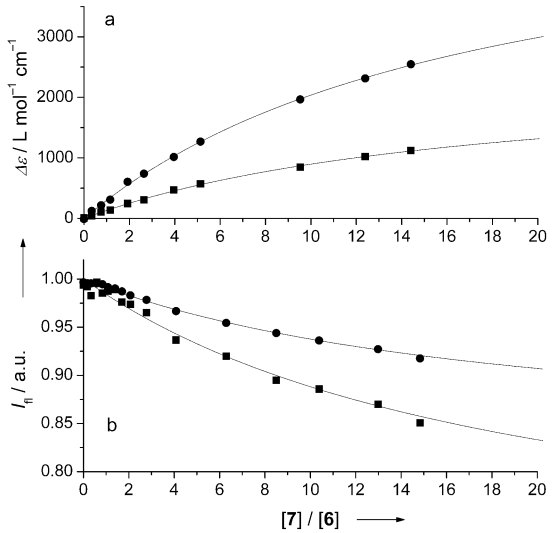

Fig. 4 (a) Changes in UV-Vis absorbance at 365 nm (circles) and 600 nm (squares) and calculated lines for naphthalene bisimide **6** ($c = 5 \times 10^{-6}$ M) in the presence of increasing amounts of melamine **7** in methylcyclohexane. (b) Changes in fluorescence intensity at the detection wavelength of 625 nm (squares) and from the integrated emission intensity (circles) for the same system. The excitation wavelength was 600 nm.

Table 2 Solubility of 1 : 1 complexes between naphthalene bisimides and melamines at a concentration of 5×10^{-5} M in MCH[a]

	3b	4	5
8a	−	−	−
8b	−	−	−
8c	−	+	+
8d	+	+	+

[a] After sonication, a clear colored solution was initially obtained (+); or the material did not dissolve at all (−).

bisimide dyes by triple hydrogen bonding to the much better soluble dialkyl melamines can promote the dissolution of the dyes, but the heterocomplexes are not stable in aliphatic solvents in the thermodynamic sense. Therefore, they behave like dispersions.

UV-Vis spectroscopic studies of these freshly prepared MCH dispersions revealed a striking difference between the assemblies containing the unsymmetrically substituted naphthalene bisimides **3b** and **4** on the one hand and those containing the symmetrically substituted compound **5** on the other hand (Fig. 5 and Fig. 6).

In Fig. 5 the absorption spectra of the assemblies of **3b**·**8d**, **4**·**8c** and **4**·**8d** are shown which reveal strong line broadening due to aggregate formation and no fluorescence. A different behavior was observed for the melamine assemblies of naphthalene bisimide **5** that showed minor spectral shifts and line broadening of the absorption band, but intense fluorescence (Fig. 6). In

Table 1 Binding constants K and Gibbs binding energies ΔG^0_{298} as determined by ^{1}H NMR, UV-Vis and fluorescence titration experiments of monotopic naphthalene bisimide **6** with various melamines

Melamine	Solvent	K/L mol^{-1}	$-\Delta G^0_{298}$/kJ mol^{-1}	δ_{min}/ppm[a]	δ_{max}/ppm[a]	Method
7	$CDCl_3$	130 ± 20[b]	12.1	8.33	15.24	NMR
8b	$CDCl_3$	90 ± 5[b]	11.1	8.32	14.10	NMR
8c	$CDCl_3$	65 ± 10[b]	10.3	8.37	15.24	NMR
7	MCH	13200 ± 2900[c]	23.5	—	—	UV-Vis
7	MCH	12400 ± 3900[c]	23.4	—	—	Fluoresence

[a] As obtained from nonlinear regression analysis for the free (δ_{min}) and the bound imide protons (δ_{max}). [b] Average of the data calculated for the imide proton and the amino proton in 2-position. [c] Average of data obtained for three different wavelengths.

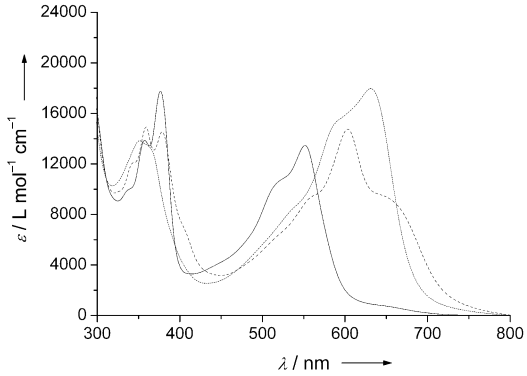

Fig. 5 UV-Vis absorption spectra of 5×10^{-5} M dispersions of naphthalene bisimide–melamine aggregates in methylcyclohexane (solid line: **3b**·**8d**; dotted line: **4**·**8c**; dashed line: **4**·**8d**).

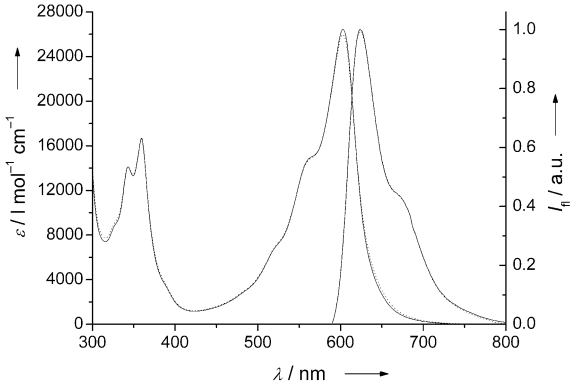

Fig. 6 UV-Vis absorption and fluorescence spectra of 5×10^{-5} M dispersions of **5**·**8c** (solid line) and **5**·**8d** (dotted line) in methylcyclohexane. The excitation wavelength was 600 nm.

addition, these dispersions are the most stable ones leading to dye precipitation only after about one day. Dilution of the self-assembled 5×10^{-5} M solutions of **5**·**8c** and **5**·**8d** to a concentration of 10^{-7} M afforded bathochromic shifts of 4 nm, which is indicative of the disassembly of hydrogen bonded species (compare Fig. 3). Examination of the MCH dispersions of **5**·**8c** and **5**·**8d** by fluorescence spectroscopy reveals an almost identical peak position and line shape as for the uncomplexed chromophores, along with a fluorescence intensity which almost reaches that of the free dye (fluorescence quantum yields $\Phi_f =$ 0.45 (**5**·**8c**) and $\Phi_f = 0.46$ (**5**·**8c**)). These observations imply that for the melamine complexes of **5** with **8c** and **8d** no substantial π–π stacking occurs between the dyes.

Taken together, these studies suggest that ditopic melamines can help to dissolve naphthalene bisimide dyes **3**–**5** at micromolar concentrations in MCH by means of hydrogen bonding. Depending on the respective combination of bisimide dye and melamine, additional π–π stacking may take place. However, in the present case no regular superstructures could be observed after evaporation of the dispersions on carbon–formvar coated copper grids by transmission electron microscopy, in contrast to perylene bisimide–melamine assemblies that we have studied previously.[6]

Scanning tunnelling microscopy

Monolayer formation from phenyloctane solutions of naphthalene bisimides **3b**, **4** and **5**, and of melamines **8b** and **8c** as well as of mixtures of **5** and **8b** were investigated by means of scanning tunnelling microscopy (STM) at the liquid/graphite interface.

Fig. 7a displays a large-scale STM image of a monolayer of dioctadecylamino-naphthalene bisimide **5** at the liquid/solid interface, spontaneously formed by physisorption after applying a drop of the 1-phenyloctane solution onto the highly oriented pyrolytic graphite (HOPG) surface. The STM image reveals not

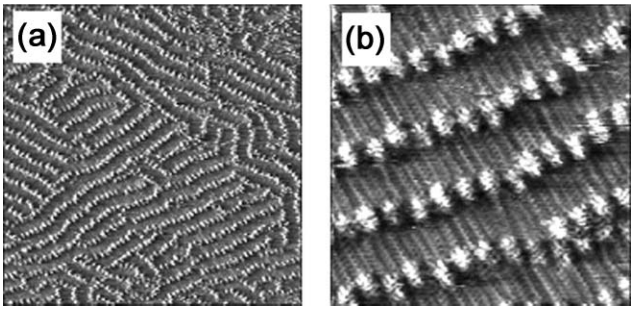

Fig. 7 (a) Large-scale and (b) small-scale STM image of a monolayer of **5** at the liquid/solid interface. Image size and scan parameters are (a) 60.0×60.0 nm^2, $I_{set} = 0.70$ nA, $V_{bias} = -0.37$ V and (b) 12.9×12.9 nm^2, $I_{set} = 0.60$ nA, $V_{bias} = -0.49$ V.

perfectly straight rows of bright spots. The latter, corresponding to a higher tunnelling probability, are the naphthalene bisimide cores and the darker area between the naphthalene bisimide rows contains the alkylamino substituents. Fig. 7b shows a small-scale submolecularly resolved STM image in which individual alkyl chains are distinguished. They progress almost parallel to one of the main symmetry axes of the substrate as revealed by imaging the graphite substrate following monolayer imaging, and the alkyl chains of adjacent rows are interdigitated. The intermolecular distance between two adjacent naphthalene bisimide units measures 10.3 ± 0.6 Å. The distance between two adjacent rows is 34 ± 3 Å. The intermolecular distance between adjacent naphthalene bisimide cores indicates hydrogen bonding and the alkyl chains are fully extended.

Interestingly, however, this compound does not form a two-dimensional crystal as the naphthalene bisimide rows are not straight. The lack of 2D crystallinity can be understood in terms of different possible motifs involving the formation of two intermolecular hydrogen bonds. The naphthalene bisimide core has two hydrogen bond acceptor–donor–acceptor (ADA) arrays as indicated in Fig. 8 (top structure). On both sites, an additional NH hydrogen bond donor unit is present at the amino functionality. Consequently, different hydrogen bonding motifs are possible as shown in the models in Fig. 8 leading to '*cis*' and '*trans*' type patterns (models a and b).[22] The type of interaction shown in model c is less probable as NMR data clearly indicate strong intramolecular hydrogen bonding between the imide carbonyl oxygen and the amino hydrogen. However, because

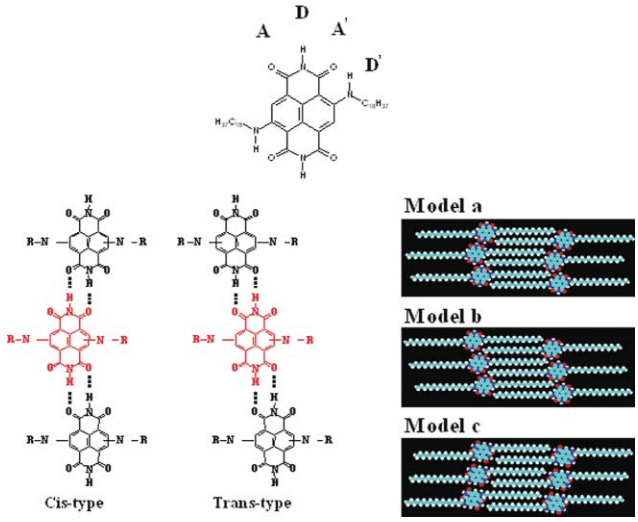

Fig. 8 Chemical structure of **5** with the marked hydrogen donor (D and D′) and acceptor (A and A′) sites. Several types of interaction are possible, leading to '*cis*' and '*trans*' patterns. CPK models a and b illustrate *cis* and *trans*-type arrangements, respectively. Model c lacks intramolecular hydrogen bonding and is unlikely to be a dominant interaction type.

'*cis*' and '*trans*' arrangements are supposed to be similar in energy (equal number of hydrogen bonds and similar interaction between the alkyl chains) it is not surprising that both motifs are observed leading to 2D non-crystalline phases.

Fig. 9a and Fig. 9b show STM images of monolayers of the unsymmetric compounds **3b** and **4** physisorbed from 1-phenyloctane on HOPG, respectively.

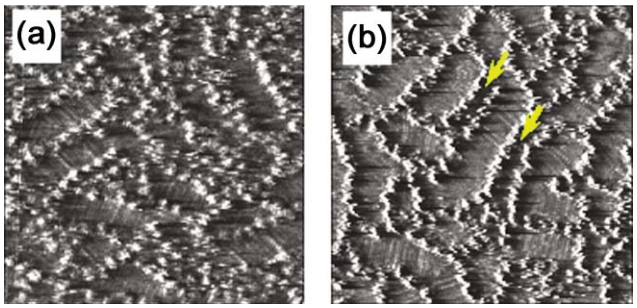

Fig. 9 STM images of monolayers of unsymmetrically substituted naphthalene bisimide derivatives physisorbed at the liquid/solid interface. (a) **3b**: Image size is 22.2 × 22.2 nm^2, scan parameters: $I_{set} = 0.70$ nA, $V_{bias} = -0.52$ V and (b) **4b**: Image size is 21.6 × 21.6 nm^2, scan parameters: $I_{set} = 0.70$ nA, $V_{bias} = -0.54$ V. The yellow arrows indicate the location of the butyl groups.

The STM images of **3b** and **4** clearly show the formation of less ordered monolayer structures compared to **5** (see Fig. 7a), although the former compounds still form rows of naphthalene bisimide cores. The distance between two adjacent naphthalene bisimide units along a row is in the order of 9.7 ± 0.8 Å for **3b** and 11.0 ± 0.5 Å for **4**. Due to pronounced disordering, an accurate determination of the intermolecular distance is not feasible. The largest distance between adjacent naphthalene bisimide rows ranges from 31 ± 1 Å for **3b** to 33 ± 1 Å for **4**, respectively, suggesting interdigitation of the octadecyl chains as found for **5**. In the case of **3b**, many defects were observed. Nevertheless, the naphthalene bisimide units seem to interact with each other, as the molecules always appear in rows. As the distance between adjacent bright spots along a row is similar to the value obtained for **5**, it is reasonable to assume that these molecules also interact by hydrogen bonding. Compound **4** forms slightly better-ordered monolayer structures than compound **3b**. However, uninterrupted rows of naphthalene bisimide functionalities are hardly longer than a few tens of nanometers. Octadecyl groups are located in the large area between rows of naphthalene bisimide groups. The smaller inter-row distance of naphthalene bisimide groups is occupied by interdigitated butyl groups, as indicated by arrows in Fig. 9b, though the inter-row distance (*ca.* 10 Å) is slightly larger than the length of fully extended amino butyl chains (*ca.* 7 Å). Clearly, the unsymmetric nature of the system leads to less ordered monolayer structures, although locally, the ordering of the molecules is definitely not random.

Fig. 10a shows an STM image of a monolayer formed from the ditopic melamine **8b**. The formation of an intermolecular hydrogen bonding network based on (DA–AD) complexes is expected. Upon applying a drop from an **8b** solution in 1-phenyloctane on HOPG, a physisorbed monolayer is formed at the liquid/solid interface. As observed in the sub-molecularly resolved STM image, **8b** forms a lamella-type monolayer structure. The lamella structure is characterized by two dark troughs which define the lamella borders, indicated by the two white arrows, a bright line in the middle of the lamella (the melamine groups), and gray lines (the alkyl chains) at both sides of the melamine groups. The alkyl chains form an angle of 70 ± 3° with respect to the long lamella axis. To each bright spot (melamine group) two alkyl chains are connected, which implies that the melamine cores are ordered in a head-to-head fashion and interact by hydrogen bonding. A few molecular models are superimposed on the STM images in Fig. 10a, and Fig. 10b shows a tentative model of the ordering of these molecules. The intermolecular distance between equivalent bright spots along a row is obtained as 9.7 ± 0.5 Å and the lamella width amounts to 55 ± 1 Å. Ditopic melamine **8b** adsorbs parallel to the surface with the molecules arranged in a head-to-head fashion with non-interdigitating alkyl chains.

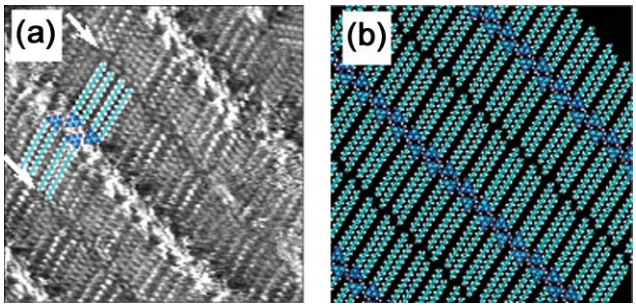

Fig. 10 (a) STM image of a monolayer of ditopic melamine **8b** at the liquid/solid interface. Upper and lower arrows indicate the lamella boundary and melamine cores, respectively. Some molecular models are superimposed on the STM picture. Image size is 10.6 × 10.6 nm^2, scan parameters: $I_{set} = 0.50$ nA, $V_{bias} = -0.55$ V. (b) Tentative molecular model.

Fig. 11a shows an STM image of a monolayer of chiral dioctadecylalanyl-derived melamine **8c** physisorbed from 1-phenyloctane on HOPG. Two arrays of bright spots (melamine groups) and alkyl chains are visible in the image. The melamine cores of **8c** are also considered to interact *via* hydrogen bonding. The intermolecular distance between melamine units along the same row is 9.7 ± 0.2 Å which is comparable to the value obtained for monolayers of **8b**. The distance between adjacent rows of melamine groups is only 36 ± 1 Å. However, the typical black troughs observed for monolayers of compound **8b** are lacking for **8c**. This is consistent with the reduced inter-row distance of 36 Å, indicating interdigitation of the alkyl chains. Moreover, only one alkyl chain per melamine unit could be observed, suggesting that one out of two alkyl chains is directed to the supernatant solution.[23] This diverse behavior is due to the different connectivity between the rigid hydrogen bonding melamine core and the alkyl chains. In the case of **8b**, the alkyl chains are directly connected to the amino groups while in **8c**, aliphatic chains are linked through a chiral methyl carboxyl moiety to the melamine core. This type of linkage might lead to a higher degree of flexibility and lower adsorption energy of the aliphatic chains. Fig. 11b and 11c show tentative top view and side view models, respectively. The invisible chains in the STM image are omitted in the top view model and colored in green in side view model.

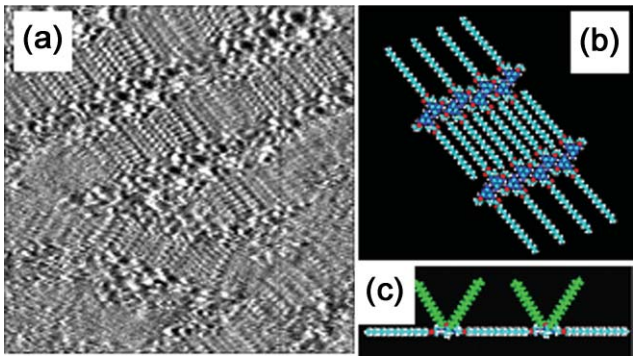

Fig. 11 (a) STM image of monolayer structure of ditopic melamine **8c** at the liquid/solid interface. Image size is 21.6 × 21.6 nm^2, scan parameters: $I_{set} = 0.80$ nA, $V_{bias} = -0.95$ V. (b) Top- and (c) side-view of tentative model. Invisible chains in an STM image are omitted in (b) and colored green in (c).

The STM observations of core substituted naphthalene bisimides and ditopic melamine derivatives indicate that the component building blocks themselves can form monolayer structures by hydrogen bonding and alkyl chain interactions. However, only two out of three hydrogen bond donor/acceptor sites are bound to the neighboring molecule. Accordingly, the question arises if mixing of naphthalene bisimides and melamines will lead to more defined supramolecular structures containing triple hydrogen bonds between the imide ADA hydrogen bonding arrays and the melamine DAD hydrogen bonding arrays. Unfortunately, mixing of the complementary components did not lead to the formation of well-defined hetero complexes at the graphite surface. All possible combinations have been investigated in different naphthalene bisimide–melamine ratios. In general, equimolar mixtures of both types of compounds led exclusively to the adsorption of the naphthalene bisimide derivatives, or separated domains of the naphthalene bisimide derivative and melamine derivative were formed at best. The naphthalene bisimide derivatives have a higher tendency to adsorb and order on the substrate than the melamine derivatives. To induce co-adsorption of the melamine derivatives, solutions of non-stoichiometric mixtures were investigated with the melamine derivative in excess. Fig. 12 shows an STM image of a monolayer obtained from a mixture of **5** and **8b** after application of a drop of phenyloctane solution of both components in a 1 : 9 molar ratio to the graphite surface. This particular mixture has been selected as both compounds have identical alkyl chain length, which might favor their 2D self-assembly on graphite, and as the pure components show a distinctly different type of pattern formation (interdigitated *vs* non-interdigitated alkyl chains). Complex formation should, therefore, give rise to patterns which can easily be distinguished from those of the pure compounds.

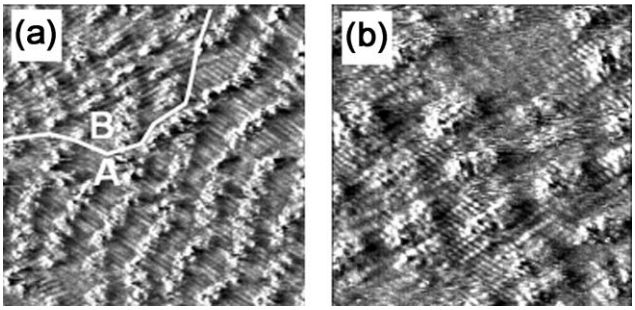

Fig. 12 STM images obtained from a mixed solution of **5** and **8b**. Image size and scan parameters are (a) 23.3 × 23.3 nm^2, $I_{set} = 0.80$ nA, $V_{bias} = -0.47$ V and (b) 10.9 × 10.9 nm^2, $I_{set} = 0.80$ nA, $V_{bias} = -0.35$ V.

In Fig. 12 two types of domains are indicated as A and B. In domain A, single bright spots are arranged in rows which are separated by interdigitated alkyl chains. The intermolecular distance of the bright spots along the row axis (*ca.* 11 Å) and between adjacent rows (*ca.* 34 Å) is in good agreement with the values obtained for the monolayer structure of **5**. Thus, the rows in domain A are considered to stem from **5**. On the other hand, the bright spots in domain B show a different type of ordering: they appear as pairs and the distance between pairs of bright spots is larger than the distance between individual spots in domain A. As the structure is different from those observed for the pure compounds, both compounds might be adsorbed in this domain. Based on the expected difference in brightness between naphthalene bisimide units and melamine units, the bright spots are tentatively assigned as the naphthalene bisimide cores. Irrespective of the exact composition and orientation of the molecules in domain B, these data illustrate that the encoding of molecules by directional hydrogen bonding to provide predefined patterns is not trivial. In some cases such as the perylene bisimide–melamine adsorbates formed from the gas phase, expectations based on the hydrogen bonding patterns were fulfilled, in other cases like here no well-ordered domains are found.

Conclusions

The selective stepwise functionalization of the core of naphthalene tetracarboxylic acid bisimides was exploited with the aim of directing hydrogen bond-mediated self-assembly of naphthalene bisimide (ADA hydrogen bonding arrays) with melamines (DAD arrays) by means of additional substituents. In the present study such complexes were investigated in solution by NMR, UV-Vis absorption and fluorescence titration studies and at the solution/graphite interface by STM. In solution, triple hydrogen bond formation between the imide groups and complementary melamines was convincingly proven by NMR studies and binding constants were measured that are in accordance with other known ADA–DAD hydrogen bonded complexes. On the other hand, no clear evidence for such arrays could be found by scanning tunnelling microscopy investigations at the liquid/solid interface. However, hydrogen bonded chains between naphthalene bisimide building blocks as well as two-dimensional patterns of ordered melamine derivatives could be observed for the individual compounds. In both cases (DA–AD) hydrogen bond complex formation contributes to the 2D organization, together with interactions between the alkyl chains. The present results lead to the conclusion that the supramolecular architectures on surfaces should not necessarily reflect the supramolecular assemblies in solution.

Experimental

General

Solvents and reagents were purchased from Merck (Darmstadt, Germany) unless otherwise stated and purified and dried according to standard procedure.[24] 2,6-Dichloronaphthalene-1,4,5,8-tetracarboxylic acid bisanhydride (**1**) was synthesized according to the literature.[13] Column chromatography was performed on silica gel (Merck Silica Gel 60, mesh size 0.2–0.5 mm). The solvents for spectroscopic studies were of spectroscopic grade and used as received; methylcyclohexane was purchased from Aldrich. UV-Vis spectra were taken on a Perkin Elmer Lambda 40P spectrometer and fluorescence spectra were measured on a SPEX Fluorolog 2 spectrofluorometer. NMR spectra were recorded on Bruker DRX 400 and Bruker AMX 500 spectrometers using TMS or the residual solvent peak as internal standard.

2,6-Dichloronaphthalene-1,4,5,8-tetracarboxylic acid bisimide (2)

A suspension of bisanhydride **1** (0.70 g, 2.1 mmol) and ammonium acetate (3.22 g, 41.8 mmol) in glacial acetic acid (20 mL) was heated to reflux for 10 min. After cooling to room temperature, the resulting colorless to slightly brown precipitate was collected on a Büchner funnel and purified by recrystallization from glacial acetic acid. Yield 0.50 g (72%); mp >350 °C; elemental analysis calcd (%) for $C_{14}H_4Cl_2N_2O_4$ (335.1): C 50.23, H 1.22, N 8.43; found C 50.14, H 1.28, N 8.42. Due to its extremely low solubility, no NMR spectrum was recorded for **2**.

2-Chloro-6-*n*-butylaminonaphthalene-1,4,5,8-tetracarboxylic acid bisimide (3a)

Bisimide **2** (0.30 g, 0.9 mmol) was stirred in *n*-butylamine (3 mL, 30 mmol) at room temperature for 24 h. The resulting violet solution was poured into 100 mL 1N HCl. After standing at room temperature for 1 h, the red precipitate was collected on

a glass filter funnel and washed with methanol. Yield 0.24 g (72%); mp >350 °C; ^{1}H NMR (500 MHz, DMSO-d$_6$, 90 °C): $\delta = 9.90$ (t, ^3J(H,H) = 5.2 Hz, 1 H, N*H*CH$_2$), 8.48 (s, 2 H, NH), 8.31 (s, 1 H, H3), 8.14 (s, 1 H, H7), 3.60 (m, 2 H, NHC*H*$_2$), 1.72 (m, 2 H, NHCH$_2$C*H*$_2$), 1.49 (m, 2 H, NHCH$_2$CH$_2$C*H*$_2$), 0.98 (t, ^3J(H,H) = 7.1 Hz, 3 H, CH$_3$); elemental analysis calcd (%) for $C_{18}H_{14}ClN_3O_4$ (371.8): C 58.15, H 3.80, N 11.30; found C 57.83, H 3.66, N 10.98.

2-Chloro-6-*n*-octadecylaminonaphthalene-1,4,5,8-tetracarboxylic acid bisimide (3b)

A suspension of bisimide **2** (0.10 g, 0.3 mmol) and *n*-octadecylamine (0.16 g, 0.6 mmol) in DMF (10 mL) was stirred at 40 °C for 4 h. The resulting red solution was stirred at room temperature for another 10 h, and then poured into a mixture of conc. HCl (10 mL) and methanol (50 mL). A red precipitate formed which was separated by centrifugation and washed with methanol. Yield 0.12 g (70%); mp >350 °C; ^{1}H NMR (500 MHz, DMSO-d$_6$, 90 °C): $\delta = 9.97$ (t, ^3J(H,H) = 5.1 Hz, 1 H, N*H*CH$_2$), 8.76 (s, 2 H, NH), 8.29 (s, 1 H, H3), 8.13 (s, 1 H, H7), 3.55 (m, 2 H, NHC*H*$_2$), 1.70 (m, 2 H, NHCH$_2$C*H*$_2$), 1.5–1.2 (m, 30 H), 0.91 (t, ^3J(H,H) = 7.3 Hz, 3 H, CH$_3$); UV-Vis (CHCl$_3$): λ_{max} (ε) = 537 (16 200), 506 (11 000, sh), 364 (15 300), 346 (12 400), 331 (8 100), 270 nm (43 100 mol^{-1} dm^3 cm^{-1}); fluorescence (CHCl$_3$): λ_{max} = 565 nm; fluorescence quantum yield: $\Phi_f = 0.57$; elemental analysis calcd (%) for $C_{32}H_{42}ClN_3O_4$ (568.2): C(67.65, H 7.45, N 7.40; found C 67.69, H 7.23, N 7.31.

2-*n*-Butylamino-6-*n*-octadecylaminonaphthalene-1,4,5,8-tetracarboxylic acid bisimide (4)

A suspension of bisimide **3a** (37.2 mg, 0.10 mmol) and *n*-octadecylamine (107.8 mg, 0.40 mmol) in *N*-methylpyrrolidone (5 mL) was stirred under argon at 150 °C for 1.5 h. After cooling to room temperature, the blue reaction mixture was poured into 1 N HCl (30 mL). The dark blue precipitate was collected on a glass filter funnel, washed with ethanol until the filtrate was clear and then washed with diethyl ether. For further purification, the obtained waxy blue solid was dissolved in hot chlorobenzene, precipitated by slow addition of methanol and separated by centrifugation. Yield 42.3 mg (70%); mp >350 °C; ^{1}H NMR (500 MHz, C$_2$D$_2$Cl$_4$, 100 °C): δ = 9.10 (br m, 2 H, N*H*CH$_2$), 8.22 (s, 2 H, NH), 8.10 (s, 2 H, H3,7), 3.47 (m, 4 H, NHC*H*$_2$), 1.77 (m, 4 H, NHCH$_2$C*H*$_2$), 1.5–1.2 (m, 32 H), 0.87 (m, 6 H, CH$_3$); UV-Vis (CHCl$_3$): λ_{max} (ε) = 620 (22 600), 578 (12 900, sh), 362 (15 900), 345 (13 100), 330 (8(500, sh), 284 nm (40(300 mol^{-1} dm^3 cm^{-1}); fluorescence (CHCl$_3$): λ_{max} = 649 nm; fluorescence quantum yield: $\Phi_f = 0.52$; elemental analysis calcd (%) for $C_{36}H_{52}N_4O_4$ (604.8): C 71.49, H 8.67, N 9.26; found C 71.61, H 8.86, N 9.24.

2,6-Di-*n*-octadecylaminonaphthalene-1,4,5,8-tetracarboxylic acid bisimide (5)

Bisimide **2** (0.20 g, 0.6 mmol) was heated under argon for 2 h in a melt of *n*-octadecylamine (2 g, 7.4 mmol) at 150 °C. After cooling to room temperature, the blue melt was dispersed in diethyl ether. The resulting suspension was poured into a mixture of conc. HCl (5 mL) and methanol (50 mL). The solid residue was collected on a Büchner funnel, washed with hot methanol and purified by recrystallization from chlorobenzene. Yield 0.25 g (52%); mp >350 °C; ^{1}H NMR (500 MHz, C$_2$D$_2$Cl$_4$, 100 °C): δ = 9.15 (br m, 2 H, N*H*CH$_2$), 8.21 (s, 2 H, NH), 8.13 (s, 2 H, H3,7), 3.45 (m, 4 H, NHC*H*$_2$), 1.76 (m, 4 H, NHCH$_2$C*H*$_2$), 1.5–1.2 (m, 60 H), 0.86 (t, ^3J(H,H) = 7.0 Hz, 6 H, CH$_3$); UV-Vis (CHCl$_3$): λ_{max} (ε) = 620 (22 200), 578 (12 300, sh), 363 (14 500), 346 (11 800), 330 (6(700, sh), 283 nm (38(700 mol^{-1} dm^3 cm^{-1}); fluorescence (CHCl$_3$): λ_{max} = 648 nm; fluorescence quantum yield: $\Phi_f = 0.53$; elemental analysis calcd (%) for $C_{50}H_{80}N_4O_4$ (801.2): C 74.96, H 10.06, N 6.99; found C 74.69, H 10.12, N 6.76.

N-(2-Ethylhexyl)-2,6-di(2-ethylhexylamino)naphthalene-1,4,5,8-tetracarboxylic acid bisimide (6)

Bisimide **2** (0.10 g, 0.3 mmol) was heated under argon in refluxing 2-ethylhexyl-amine (5 mL) at 190 °C for 7 h. The dark blue reaction mixture was poured into a mixture of conc. HCl (20 mL) and methanol (100 mL). The blue precipitate was collected on a Büchner funnel, washed with methanol and extracted with dichloromethane (3 × 20 mL). The combined extracts were dried over NaCl, concentrated and subjected to column chromatography (dichloromethane–methanol = 98 : 2, silica gel). The product was precipitated from the concentrated eluent by addition of methanol and separated by centrifugation. Yield 35 mg (18%); mp 126 °C; ^{1}H NMR (400 MHz, CDCl$_3$, 25 °C, TMS): δ = 9.48 (t, ^3J(H,H) = 5.2 Hz, 1 H, N*H*CH$_2$), 9.20 (t, ^3J(H,H) = 5.0 Hz, 1 H, N*H*CH$_2$), 8.37 (s, 1 H, NH), 8.18 (s, 1 H, H7), 8.13 (s, 1 H, H3), 4.13 (m, 2 H, NC*H*$_2$), 3.42 (m, 4 H, NHC*H*$_2$), 1.94 (m, 1 H, NCH$_2$C*H*), 1.72 (m, 2 H, NHCH$_2$C*H*), 1.5–1.2 (m, 24 H), 0.93 (m, 18 H, CH$_3$); UV-Vis (CH$_2$Cl$_2$): λ_{max} (ε) = 618 (22 400), 576 (11(700, sh), 366 (12(500), 347 (10(000), 331 (5(000, sh), 282 nm (44(900 mol^{-1} dm^3 cm^{-1}); fluorescence (CH$_2$Cl$_2$): λ_{max} = 645 nm; fluorescence quantum yield: $\Phi_f = 0.54$; elemental analysis calcd (%) for $C_{38}H_{56}N_4O_4$ (632.9): C 72.12, H 8.92, N 8.85; found C 71.97, H 8.95, N 8.81.

Preparation of naphthalene bisimide–melamine complexes

Appropriate amounts of stock solutions of a naphthalene bisimide (10^{-4} mol L^{-1} in CHCl$_3$) and a melamine (10^{-3} mol L^{-1} in CHCl$_3$–methylcyclohexane 1 : 1) were combined in a flask, and the solvent was evaporated under reduced pressure. The resulting colored film was dissolved in methylcyclohexane by sonication for 2 min and again the solvent was evaporated. This procedure was repeated at least twice to ensure complete removal of chloroform. The dispersions obtained were stable for several hours.

^{1}H NMR titration experiments

NMR titrations were performed for 1×10^{-3} mol L^{-1} constant naphthalene imide receptor (**6**) concentration at a temperature of 298 K. Aliquots of a guest solution (melamine receptor concentration 3×10^{-2} mol L^{-1}, containing 1×10^{-3} mol L^{-1} host receptor concentration) were subsequently added to the NMR tube containing an initial volume of 350 μL host solution. After each addition, a spectrum was recorded. For all investigated systems, a sufficiently sharp peak was observed for the imide proton throughout the experiment. The association constants were determined by nonlinear least-squares regression analysis from the change in chemical shift of the imide proton and the proton of the amino function in 2-position.[18]

UV-Vis titration experiments

Titrations were performed at 5×10^{-6} mol L^{-1} constant host concentration at room temperature. Two 1 cm quartz cuvettes with 1500 μL host solution and 1500 μL pure solvent were placed in a double beam spectrophotometer. Guest solutions of 10^{-4} mol L^{-1} were prepared in host solution and in pure solvent. Aliquots of these solutions were added to the cuvette with the host solution and in the reference cuvette, respectively, and a spectrum was recorded after each addition. The association constants were determined by nonlinear least-squares regression analysis from the absorbance change at several wavelengths.[18]

Fluorescence measurements

Fluorescence measurements were done with a calibrated SPEX Fluorolog 2 spectrofluorometer, and all spectra were corrected.

The fluorescence quantum yields were determined by the optically dilute method[25] using *N*,*N*′-di(2,6-diisopropylphenyl)-1,6,7,12-tetraphenoxyperylene-3,4–9,10-tetracarboxylic acid bisimide as reference (Φ_f,$CHCl_3 = 0.96$).[26] The refractive indices of the solvents used in the quantum yield calculations were obtained from the CRC handbook.[27] The given quantum yields are averaged from values at three excitation wavelengths around the absorption maximum (standard deviation $\sigma = 2$–3%). All solutions were prepared from air-saturated solvents.

Owing to the high optical densities of the solutions required for aggregate formation, fluorescence measurements on these samples were not performed using the conventional right angle setup, but the front face illumination technique on a 1 mm cell in order to minimize re-absorption.[28]

Fluorescence titration studies

Titrations were performed at 5×10^{-6} mol L^{-1} constant host concentration at room temperature. A guest solution of 1×10^{-4} mol L^{-1} was prepared in host solution and added in small aliquots to the cell with the host solution (initial volume 1500 μL). Spectra with excitation wavelengths of 600 and 610 nm were recorded after each addition. The association constants were determined by nonlinear least-squares regression analysis from the fluorescence intensity change at different wavelengths as well as the integrated fluorescence intensity.[18]

Electron microscopy

A drop of a 5×10^{-5} M dispersion of the naphthalene bisimide–melamine assemblies in methylcyclohexane was evaporated on a formvar–carbon coated copper grid (300 mesh). The specimens were examined in a Zeiss EM 10 transmission electron microscope operating at 80 kV. For freeze-fracture experiments, a drop of a 5×10^{-5} M dispersion of the naphthalene bisimide–melamine aggregates in methylcyclohexane was put on a copper grid (300 mesh, without coating) between two copper platelets and cooled in liquid nitrogen. After 5 min, the sample was mounted on a Balzers freeze-fracture stage which was thermostatted at −130 °C. The surrounding chamber was evacuated, and the copper platelets were torn apart. Then the specimen was sputtered with platinum at an angle of 45° and subsequently with carbon and allowed to reach room temperature. The samples were examined under the conditions described above.

Scanning tunnelling microscopy

The STM investigation was carried out at the solid/liquid interface using a Discoverer scanning tunnelling microscope (Topometrix) along with an external pulse/function generator (8111A, Hewlett Packard). The Pt–Ir (80 : 20%) tips were prepared from a 0.2 mm thick wire by electrochemical etching using a solution of NaCN (6 N) + KOH (2 N). The sample solutions in 1-phenyloctane have been applied to the basal plane of the freshly cleaved highly oriented pyrolitic graphite (HOPG) substrate. The lattice of the underlying HOPG has been monitored during the measurements by simply changing the tunnelling parameters; this permitted the calibration of the piezo in the *xy* plane *in situ*. STM current images in the variable current mode (constant height) with a submolecular resolution have been recorded using average tunnelling currents I(t) ranging from 0.3 to 0.8 nA, and a voltage V(t) ranging from −0.2 to −1.2 V (sample negative). All STM images contain raw data and have not been subjected to any manipulation or image processing.

Acknowledgements

We cordially thank the Deutsche Forschungsgemeinschaft (grant Wu 317/5-1), the Fonds der Chemischen Industrie, and the Belgian Federal Science Policy through IAP-V-03 for financial support. AM thanks KU Leuven for a fellowship. SDF is a postdoctoral fellow of the Fund for Scientific Research Flanders.

References

1 (*a*) D. Gust, T. A. Moore and A. L. Moore, *Acc. Chem. Res.*, 2001, **34**, 40–48; (*b*) A. R. Harriman, *Photochemistry*, 1998, **29**, 425–452, and references therein.
2 (*a*) V. Balzani, F. Scandola, *Supramolecular Photochemistry*, Ellis Horwood Ltd., Chichester, 1991; (*b*) J. Kim and T. M. Swager, *Nature*, 2001, **411**, 1030–1034; (*c*) L. Schmidt-Mende, A. Fechtenkötter, K. Müllen, E. Moons, R. H. Friend and J. D. MacKenzie, *Science*, 2001, **293**, 1119–1122.
3 (*a*) J. A. Theobald, N. S. Oxtoby, M. A. Phillips, N. R. Champness and P. H. Beton, *Nature*, 2003, **424**, 1029–1031; (*b*) C. Joachim, J. K. Gimzewski and A. Aviram, *Nature*, 2000, **408**, 541–548; (*c*) F. Jäckel, M. D. Watson, K. Müllen and J. P. Rabe, *Phys. Rev. Lett.*, 2004, **92**, 188–303.
4 F. Würthner, *Chem. Commun.*, 2004, 1564–1579.
5 (*a*) C. W. Struijk, A. B. Sieval, J. E. J. Dakhorst, M. Van Dijk, P. Kimkes, R. B. M. Koehorst, H. Donker, T. J. Schaafsma, S. J. Picken, A. M. van de Craats, J. M. Warman, H. Zuilhof and E. J. R. Sudhölter, *J. Am. Chem. Soc.*, 2000, **122**, 11057–11066; (*b*) C. D. Dimitrakopoulos and P. R. L. Malenfant, *Adv. Mater.*, 2002, **14**, 99–117; (*c*) A. Yakimov and S. R. Forrest, *Appl. Phys. Lett.*, 2002, **80**, 1667–1669; (*d*) Z. Chen, M. G. Debije, T. Debaerdemaeker, P. Osswald and F. Würthner, *ChemPhysChem*, 2004, **5**, 137–140; (*e*) F. Würthner, *Angew. Chem., Int. Ed.*, 2001, **40**, 1037–1039.
6 (*a*) F. Würthner, C. Thalacker and A. Sautter, *Adv. Mater.*, 1999, **11**, 754–758; (*b*) F. Würthner, C. Thalacker, A. Sautter, W. Schärtl, W. Ibach and O. Hollricher, *Chem. Eur. J.*, 2000, **6**, 3871–3886; (*c*) C. Thalacker and F. Würthner, *Adv. Funct. Mater.*, 2002, **12**, 209–218; (*d*) A. P. H. J. Schenning, J. v. Herrikhuyzen, P. Jonkheijm, Z. Chen, F. Würthner and E. W. Meijer, *J. Am. Chem. Soc.*, 2002, **124**, 10252–10253.
7 (*a*) F. Würthner, A. Sautter, D. Schmid and P. J. A. Weber, *Chem. Eur. J.*, 2001, **7**, 894–902; (*b*) F. Würthner and A. Sautter, *Org. Biomol. Chem.*, 2003, **1**, 240–243; (*c*) C.-C. You and F. Würthner, *J. Am. Chem. Soc.*, 2003, **125**, 9716–9725; (*d*) R. Dobrawa and F. Würthner, *Chem. Commun.*, 2002, 1878–1879; (*e*) F. Würthner, C.-C. You and C. R. Saha-Möller, *Chem. Soc. Rev.*, 2004, **33**, 133–146.
8 (*a*) C. Ludwig, B. Gompf, J. Petersen, R. Strohmaier and W. Eisenmenger, *Z. Phys. B: Condens. Matter*, 1994, **93**, 365–373; (*b*) B. Uder, C. Ludwig, J. Petersen, B. Gompf and W. Eisenmenger, *Z. Phys. B: Condens. Matter*, 1995, **97**, 389–390.
9 D. L. Keeling, N. S. Oxtoby, C. Wilson, M. J. Humphry, N. R. Champness and P. H. Beton, *Nano Lett.*, 2003, **3**, 9–12.
10 F. Würthner, S. Ahmed, C. Thalacker and T. Debaerdemaeker, *Chem. Eur. J.*, 2002, **8**, 4742–4750; for earlier work on amino-substituted naphthaline bisimides where the color but not the fluorescence properties have been described see: (*a*) E. Bonnet, P. Gangneux and E. Maréchal, *Bull. Soc. Chim. Fr.*, 1976, 504–507; (*b*) E. F. Bondarenko, V. A. Shigalevskii and G. A. Yugai, *Zh. Org. Khim.*, 1982, **18**, 610–615.
11 An example for supramolecular assemblies of unsubstituted naphthalene bisimide with melamines can be found in: N. Kimizuka, T. Kawasaki, K. Hirata and T. Kunitake, *J. Am. Chem. Soc.*, 1995, **117**, 6360–6361.
12 (*a*) J. A. Zerkowski, J. C. MacDonald, C. T. Seto, D. A. Wierda and G. M. Whitesides, *J. Am. Chem. Soc.*, 1994, **116**, 2382–2391; (*b*) J. A. Zerkowski and G. M. Whitesides, *J. Am. Chem. Soc.*, 1994, **116**, 4298–4304; (*c*) J. A. Zerkowski, J. P. Mathias and G. M. Whitesides, *J. Am. Chem. Soc.*, 1994, **116**, 4305–4315; (*d*) J. C. MacDonald and G. M. Whitesides, *Chem. Rev.*, 1994, **94**, 2383–2420.
13 H. Vollmann, H. Becker, M. Corell and H. Streeck, *Liebigs Ann. Chem.*, 1937, **531**, 1–159.
14 E. F. Bondarenko and V. A. Shigalevskii, *Zh. Org. Khim.*, 1983, **19**, 2377–2382; E. F. Bondarenko and V. A. Shigalevskii, *J. Org. Chem. USSR (Engl. Transl.)*, 1983, **19**, 2079–2083.
15 (*a*) F. H. Beijer, R. P. Sijbesma, H. Kooijman, A. L. Spek and E. W. Meijer, *J. Am. Chem. Soc.*, 1998, **120**, 6761–6769; (*b*) J. L. Sessler, C. T. Brown, D. O'Connor, S. L. Springs, R. Wang, M. Sathiosatham and T. Hirose, *J. Org. Chem.*, 1998, **63**, 7370–7374; (*c*) F. Würthner and S. Yao, *J. Org. Chem.*, 2003, **68**, 8943–8949.
16 The weakness of this type of triple hydrogen bonds has been explained by unfavorable secondary electrostatic interactions, see (*a*) J. Pranata, S. G. Wierschke and W. L. Jorgensen, *J. Am. Chem. Soc.*, 1991, **113**, 2810–2811; (*b*) J. Sartorius and H.-J. Schneider, *Chem. Eur. J.*, 1996, **2**, 1446.
17 (*a*) E. E. Simanek, X. Li, I. S. Choi and G. M. Whitesides, in *Comprehensive Supramolecular Chemistry Vol. 9*, ed. J. L. Atwood,

J. E. D. Davies, D. D. MacNicol and F. Vögtle, Pergamon, Oxford, 1996, pp. 595–621; (*b*) G. M. Whitesides, E. E. Simanek and J. P. Mathias, *Acc. Chem. Res.*, 1995, **28**, 37–44; (*c*) M. Mammen, E. E. Simanek and G. M. Whitesides, *J. Am. Chem. Soc.*, 1996, **118**, 12614–12623; (*d*) L. J. Prins, D. N. Reinhoudt and P. Timmerman, *Angew. Chem., Int. Ed.*, 2001, **40**, 2382–2426; (*e*) L. J. Prins, J. J. Verhage, F. de Jong, P. Timmermann and D. N. Reinhold, *Chem. Eur. J.*, 2002, **8**, 2302–2313.

18 (*a*) K. A. Connors, *Binding Constants*, Wiley & Sons, New York, 1987; (*b*) C. S. Wilcox, in *Frontiers of Supramolecular Chemistry and Photochemistry*, ed. H. J. Schneider and H. Dürr, VCH, Weinheim, 1991, pp. 123–143; (*c*) A. P. Bisson, C. A. Hunter, J. C. Morales and K. Young, *Chem. Eur. J.*, 1998, **4**, 845–851.

19 *Origin 5.0*, Microcal Software, Inc., Northampton, 1997.

20 In MCH the absorption maximum is shifted by about 12 nm to lower wavelengths with respect to chloroaliphatic solvents, indicating a higher dependence of the optical properties of core-substituted naphthalene bisimides on solvent effects than for perylene bisimides.

21 The influence of substituent on rotational barriers in trisubstituted triazines is discussed in (*a*) A. R. Katritzky, D. C. Oniciu, I. Ghiviriga and R. A. Barcock, *J. Chem. Soc., Perkin Trans. 2*, 1995, 785–792; (*b*) A. R. Katritzky, I. Ghiviriga, P. J. Steel and D. C. Oniciu, *J. Chem. Soc., Perkin Trans. 2*, 1996, 443–447.

22 Two more possibilities arise if we consider the position of the NH-alkyl chains in space. However, as these could not be resolved by STM they are not discussed here. Nevertheless, they constitute another reason for the observed disorder.

23 (*a*) Y. Kaneda, M. E. Stawasz, D. L. Sampson and B. A. Parkinson, *Langmuir*, 2001, **17**, 6185–6195; and references therein.

24 D. D. Perrin, W. L. F. Armarego, *Purification of Laboratory Chemicals, 2nd edn.*, Pergamon Press, Oxford, 1980.

25 J. R. Lakowicz, *Principles of Fluorescence Spectroscopy, 2nd edn.*, Kluwer Academic/Plenum Publishers, New York, 1999, pp. 52–53.

26 (*a*) G. Seybold and G. Wagenblast, *Dyes Pigm.*, 1989, **11**, 303–317; (*b*) R. Gvishi, R. Reisfeld and Z. Burshtein, *Chem. Phys. Lett.*, 1993, **213**, 338–344.

27 *CRC Handbook of Chemistry and Physics, 72nd edn.*, ed. D. R. Lide CRC Press, Boca Raton, FL, 1991.

28 J. R. Lakowicz, *Principles of Fluorescence Spectroscopy, 2nd edn.*, Kluwer Academic/Plenum Publishers, New York, 1999, pp. 53–55.